

Article

The Female-Biased General Odorant Binding Protein 2 of *Semiothisa cinerearia* Displays Binding Affinity for Biologically Active Host Plant Volatiles

Jingjing Tu ^{1,2}, Zehua Wang ¹, Fan Yang ¹ , Han Liu ¹, Guanghang Qiao ¹, Aihuan Zhang ² and Shanning Wang ^{1,*} 

- ¹ Key Laboratory of Environment Friendly Management on Fruit and Vegetable Pests in North China (Coconstructed by the Ministry and Province), Ministry of Agriculture and Rural Affairs, Institute of Plant Protection, Beijing Academy of Agriculture and Forestry Sciences, Beijing 100097, China; 15910506265@163.com (J.T.); wangzehua200707@163.com (Z.W.); evelynyangfan@163.com (F.Y.); 15230451215@163.com (H.L.); qghang98@126.com (G.Q.)
- ² College of Bioscience and Resources Environment, Beijing University of Agriculture, Beijing 102206, China; zhangaihuan@126.com
- * Correspondence: wangshanning@yeah.net

Simple Summary: The moth *Semiothisa cinerearia* (Lepidoptera: Geometridae) is a major pest of Chinese scholar trees (*Sophora japonica* L.). Olfaction is very important for insects to locate host plants and oviposition sites. Here, we identified the binding abilities of ScinGOBP2 for host plant volatiles using fluorescence-based competitive binding assays. We also confirmed the key amino acid residues that bind to plant volatiles in ScinGOBP2 via three-dimensional structure modeling and molecular docking. The ScinGOBP2 ligands had attractive or repellent behavioral effects on *S. cinerearia* for oviposition. Overall, ScinGOBP2 may play important roles in detecting host plant volatiles, and ScinGOBP2 ligands could be used as candidate olfactory regulators for the management of *S. cinerearia*.



Citation: Tu, J.; Wang, Z.; Yang, F.; Liu, H.; Qiao, G.; Zhang, A.; Wang, S. The Female-Biased General Odorant Binding Protein 2 of *Semiothisa cinerearia* Displays Binding Affinity for Biologically Active Host Plant Volatiles. *Biology* **2024**, *13*, 274. <https://doi.org/10.3390/biology13040274>

Academic Editor: Jim O. Vigoreaux

Received: 20 March 2024

Revised: 13 April 2024

Accepted: 16 April 2024

Published: 18 April 2024



Copyright: © 2024 by the authors. Licensee MDPI, Basel, Switzerland. This article is an open access article distributed under the terms and conditions of the Creative Commons Attribution (CC BY) license (<https://creativecommons.org/licenses/by/4.0/>).

Abstract: Herbivorous insects rely on volatile chemical cues from host plants to locate food sources and oviposition sites. General odorant binding proteins (GOBPs) are believed to be involved in the detection of host plant volatiles. In the present study, one GOBP gene, *ScinGOBP2*, was cloned from the antennae of adult *Semiothisa cinerearia*. Reverse-transcription PCR and real-time quantitative PCR analysis revealed that the expression of *ScinGOBP2* was strongly biased towards the female antennae. Fluorescence-based competitive binding assays revealed that 8 of the 27 host plant volatiles, including geranyl acetone, decanal, *cis*-3-hexenyl n-valerate, *cis*-3-hexenyl butyrate, 1-nonene, dipentene, α -pinene and β -pinene, bound to ScinGOBP2 ($K_D = 2.21$ – $14.94 \mu\text{M}$). The electrical activities of all eight ScinGOBP2 ligands were confirmed using electroantennography. Furthermore, oviposition preference experiments showed that eight host volatiles, such as decanal, *cis*-3-hexenyl n-valerate, *cis*-3-hexenyl butyrate, and α -pinene, had an attractive effect on female *S. cinerearia*, whereas geranyl acetone, 1-nonene, β -pinene, and dipentene inhibited oviposition in females. Consequently, it can be postulated that ScinGOBP2 may be implicated in the perception of host plant volatiles and that ScinGOBP2 ligands represent significant semiochemicals mediating the interactions between plants and *S. cinerearia*. This insight could facilitate the development of a chemical ecology-based approach for the management of *S. cinerearia*.

Keywords: *Semiothisa cinerearia*; general odorant binding protein; ligand-binding spectrum; molecular docking; electrophysiological; behavioral responses

1. Introduction

Herbivorous insects primarily depend on their sense of smell to distinguish chemical signals released by host plants, enabling them to locate food sources and choose suitable

places for laying eggs within complex chemical environments [1–3]. These chemical cues are presumably perceived by specialized olfactory sensilla, predominantly located on the insect antennae. The structure of olfactory sensilla is punctuated with numerous pores, forming a cavity filled with aqueous lymph. This cavity harbors olfactory receptor neurons' (ORNs) dendritic branches and is enriched with small soluble proteins. Odorants present in the environment enter sensilla via cuticular pores, are dissolved in the sensillar lymph, initiate the activation of ORNs, and ultimately induce various behavioral responses [4–6]. Odorant binding proteins (OBPs) are the main types of soluble binding proteins involved in the binding, solubilizing, and transport of hydrophobic odorants across the aqueous environment of the sensillar lymph to odorant receptors in the dendritic membranes of ORNs [7–9].

In insects, OBPs are divided into different subfamilies based on their sequence and the tissue in which they are expressed [8,10,11]. Pheromone binding proteins (PBP) and general odorant binding proteins (GOBPs) in Lepidoptera form a distinct subclass; they are abundant in moth antennae and are associated with chemosensory sensilla [12–14]. In Lepidoptera species, PBPs are believed to function in perception of female sex pheromones, while GOBPs are thought to be involved in interacting with plant odorants. For instance, GOBP2 of *Agrotis ipsilon* [15], GOBP2 of *Spodoptera frugiperda* [16], and GOBP1-2 of *Orthaga achatina* [17] can strongly bind to the corresponding host plant volatiles. Recently, genome editing via CRISPR–Cas9 was used to verify that the GOBPs of *S. litura* participate and *Conogethes punctiferalis* in the detection of host odorants in vivo [18,19]. These findings indicate that moth GOBPs play important roles in determining the location of the host plant. However, it has been reported in some studies that GOBPs can bind sex pheromones, and they are also thought to function in the perception of sex pheromones [15,20,21]; however, further in vivo functional studies are needed [18,22].

Semiothisa cinerearia (Bremer et Gray), which belongs to the subfamily Ennominae (Lepidoptera: Geometridae), is a forestry pest that attacks *Sophora japonica*. *S. japonica*, which is native to China and known as the Chinese scholar tree, widely cultivated in urban greenbelts in China [23,24]. In recent years, Chinese scholar trees have been severely damaged by *S. cinerearia* in northern China. To control *S. cinerearia*, excessive amounts of insecticides have been applied, which has had negative effects on the ecosystem. To devise environmentally friendly methods of pest control, such as by regulating olfactory behavior, many chemosensory genes, including 26 OBP genes [25,26] that await functional characterization, have been identified in *S. cinerearia*.

In the present study, we investigated the function of the female-biased GOBP, ScinGOBP2, in the detection of host plant volatiles by profiling the expression of *ScinGOBP2* transcripts in various tissues from male and female moths using reverse transcription PCR (RT-PCR) and quantitative real-time PCR (qRT-PCR). ScinGOBP2 was expressed in vitro to evaluate its binding affinity for 27 volatiles from *S. japonica* volatiles via fluorescence binding assays. Additionally, homology modeling and molecular docking were utilized to identify the essential amino acids in ScinGOBP2 involved in ligand binding. The biological activity of the ScinGOBP2 ligands was further validated through electroantennography (EAG) and two-choice oviposition preference assays.

2. Materials and Methods

2.1. Insect Culture, Tissue Collection, RNA Extraction, and cDNA Synthesis

Pupae of *S. cinerearia* were harvested from soil beneath Chinese scholar trees in the suburbs of Beijing, China. The pupae were maintained in a rearing cage at 25 ± 1 °C and $60 \pm 10\%$ relative humidity with a 16L:8D photoperiod. The emerged adults were fed a 10% sucrose solution. For *ScinGOBP2* gene cloning and tissue expression profiling, male antennae, female antennae, heads (without antennae), legs and bodies (a mixture of thoraxes, abdomens, and wings) were excised from 1- to 3-day-old adult moths. All samples were immediately frozen in liquid nitrogen and subsequently stored at -80 °C for RNA extraction. Total RNA was isolated from the samples using TRIzol reagent (Invitrogen,

Carlsbad, CA, USA), adhering to the protocol provided by the manufacturer. The integrity and quantity of the extracted RNA samples were verified through 1.2% agarose gel electrophoresis and measurement with a NanoPhotometer N60 (Implen, München, Germany), respectively. cDNA was generated from 2 µg of RNA for each sample using the Fast Quant RT Kit (with gDNase) (Tiangen, Beijing, China), according to the manufacturer's instructions, and this cDNA served as the template for subsequent gene cloning and RT-PCR and qRT-PCR analyses.

2.2. Gene Cloning and Sequence Analysis

Drawing on the adult *S. cinerearia* antennal transcriptome data [25], the open reading frame (ORF) of *ScinGOBP2* was cloned using gene specific primers (Table S1). PCR was performed in 25 µL reactions containing 2 × Premix Taq™ (12.5 µL; Biomed, Beijing, China), forward primers (10 µM), reverse primers (10 µM), the antennal cDNA template (1 µL), and ddH₂O (9.5 µL). PCR was conducted as follows: 94 °C for 4 min, followed by 30 cycles of 94 °C for 30 s, annealing at 55 °C for 30 s, and extension at 72 °C for 45 s. The final extension step was at 72 °C for 5 min. The PCR products were checked by using 1.2% agarose gel and subsequently verified via DNA sequencing.

The signal peptides were predicted using the SignalP5.0 server (<http://www.cbs.dtu.dk/services/SignalP/>) (accessed on 24 June 2022). The isoelectric points (IPs) and molecular weights (MWs) were calculated using the ExPASy Proteomics Server (<https://www.ExPASy.org/>) (accessed on 24 June 2022). Sequences were aligned using ClustalW Multiple Alignment in BioEdit version 7.1.3.0.

2.3. RT-PCR and qRT-PCR

The primers used for RT-PCR and qRT-PCR analyses were designed with Primer 3 (<http://primer3.ut.ee/>) (accessed on 26 November 2022) (Table S1).

The differential expression of *ScinGOBP2* across various tissues in both male and female moths was examined using RT-PCR, employing Taq DNA polymerase (Biomed, Beijing, China) for the reactions. For each 25 µL reaction, 200 ng of cDNA from different tissues served as a template. The PCR was conducted with the same cycling conditions outlined above. *β-Actin* from *S. cinerearia* was used as the control gene to test the integrity of the cDNA. The PCR products were checked by using 1.2% agarose gels, and a randomly chosen PCR product was sequenced to confirm its identity.

The relative transcript abundance of *ScinGOBP2* in different tissues was determined via qRT-PCR on an ABI Prism 7500 Fast Detection System (Applied Biosystems, Carlsbad, CA, USA). Two endogenous genes, *β-actin* and *TBP* (TATA-binding protein-associated factor 172), were used for normalization. The efficiency of the primers was calculated by analyzing the standard curves with a 5-fold dilution series of the female antennal cDNA template. The 25 µL reactions contained 2 × SuperReal PreMix Plus (12.5 µL; TianGen, Beijing, China), 50 × ROX Reference Dye (0.5 µL), forward primers (7.5 µM), reverse primers (7.5 µM), sample cDNA (200 ng), and ddH₂O (8.5 µL). The qRT-PCR cycling parameters consisted of 95 °C for 15 min, followed by 40 cycles of 95 °C for 10 s and 60 °C for 32 s. Melting curves were constructed by raising the temperature to 95 °C in 0.35 °C/s increments. Non-template controls were included in each experiment. Each qRT-PCR experiment was carried out in three biological replicates and three technical replicates. The comparative cycle threshold ($2^{-\Delta\Delta CT}$) method was used for measuring the relative transcript levels in each tissue.

2.4. Recombinant *ScinGOBP2* Expression

The chemically synthesized cDNA was cloned and inserted into pET30a (+) vector by Taihe (Beijing, China). The expression plasmid was transformed into Rosetta (DE3) competent cells. The protein was expressed in LB broth at 18 °C for 16 h through induction with 1 mM isopropyl-β-D-thiogalactopyranoside. The bacterial cells were harvested via centrifugation and resuspended in PBS (pH 7.4, 10 mM). After sonication and centrifugation,

the recombinant protein was detected in both the supernatant and inclusion bodies. The supernatant was applied to the Ni column (GenScript, Nanjing, China) to purify the protein. The His-tag was removed using recombinant enterokinase (Yaxin, Shanghai, China), adhering to the manufacturer's guidelines. The purified ScinGOBP2 was dialyzed in PBS, and its concentration was then measured using the Bradford assay.

2.5. Fluorescence-Based Competitive Binding Assays

A total of 27 volatile compounds were selected for a fluorescence-based competitive binding assay based on previously reported information for *S. cinerearia* host plants [27]. This experiment was performed on a spectrofluorometer F-380 (Tianjin, China) using slits of 10 nm and a light path of 1 cm. The fluorescent probe N-phenyl-1-naphthylamine (1-NPN) was excited at 337 nm, and emissions were recorded between 390 and 530 nm. The affinity of 1-NPN for ScinGOBP2 was measured by titrating a 2 μ M solution of the protein with aliquots of 1 mM 1-NPN in methanol to final concentrations of 1–16 μ M. The dissociation constants of 1-NPN and the proteins were calculated using the software GraphPad Prism 8.0. Competitive binding was measured via the titration of the protein/1-NPN (both at 2 μ M) mixture by adding aliquots of 1 mM of methanol solution of ligand to final concentrations of 2–30 μ M. Dissociation constants of the competitors were calculated using the equation $K_D = IC_{50}/(1 + [1-NPN]/K_{1-NPN})$, where IC_{50} represents the ligand concentration achieving a 50% decrease in 1-NPN's initial fluorescence intensity, [1-NPN] represents the free concentration of 1-NPN, and K_{1-NPN} represents the dissociation constant of the complex ScinGOBP2/1-NPN. These procedures were replicated three times, except for the ligand interactions that showed no significant binding, which were assessed in singular assays.

2.6. Three-Dimensional Modeling of ScinGOBP2 and Ligand Docking

A three-dimensional (3D) structure of ScinOBP2 was constructed using AlphaFold2 by submitting the amino acid sequence to the Beijing Super Cloud Computing Center (Beijing, China). The 3D structure was then subjected to molecular dynamics (MD) simulation using the Amber22 and AMBER ff19SB force fields for energy minimization, resulting in the refinement of its structure. The qualities of the optimized models were evaluated using the ERRAT and PROCHECK programs. The ligands were subjected to 3D optimization in ChemDraw 3D (23.0) and refined via energy minimization. Molecular docking was performed using AutoDock Vina (4.2.6). The top models were selected according to the lowest free binding energy (kcal/mol) and visually analyzed using PyMOL (2.5.5).

2.7. Electrophysiological Recordings

Electroantennogram recordings were carried out to measure the antennal responses of *S. cinerearia* to ScinGOBP2 ligands. The antennae of *S. cinerearia* adults were carefully removed from the base, and the tips were carefully cut off. The prepared antennae were affixed to electrode holders using conductive electrode gel. Subsequently, a 10 μ L aliquot of the test compound (10 μ g/ μ L, diluted in paraffin oil) was applied to a strip of filter paper. This strip was then placed into a 1000 μ L pipette tip, serving as a cartridge. The test cartridge was connected to a stimulus controller (CS-55; Syntech, Kirchzarten, Germany) that delivered a 0.5 s stimulus every 30 s at a constant flow rate of 10 mL/s. Antennal signals were recorded using an EAG Pro system (Syntech). In all the experiments, antennae were exposed to a solvent control (paraffin oil) at the beginning and end of a series of sample measurements. Test stimuli were presented in a randomized sequence, interspersed between two control puffs. The EAG responses to the test odors were adjusted by subtracting the mean amplitude of the two control signals. EAG responses were measured from a cohort of twelve insects, each with different antennae ($n = 12$).

2.8. Two-Choice Oviposition Preference Assay

The oviposition preference of female *S. cinerearia* for the ScinGOBP2 ligands was assessed in a screened enclosure (length/width/height = 86 cm:46 cm:48 cm). To ensure mating of all the female moths, newly emerged males and females were cohabitated in a rearing enclosure (30 cm × 30 cm × 30 cm) at a sex ratio of 1:2 for a period of 2 days. Mated females for subsequent experiments were randomly selected from this enclosure. Each screened cage housed five gravid females. For adult nourishment, a small Petri dish containing 10% honey solution was positioned at the cage’s base center. Test compounds (100 µg, diluted in paraffin oil) or the solvent control (paraffin oil) were applied to a cotton ball, which was then affixed to the opposite inner sides of the cage. After 48 h, the number of eggs deposited on the gauze on both the treatment and control sides was counted. The oviposition preference index was determined using the formula $(T - C)/(T + C)$, where T represents the egg count on the treatment side and C represents the count on the control side. Each experiment was replicated eight times.

2.9. Statistical Analysis

The statistical analysis of the data was conducted using SPSS 18.0 and GraphPad Prism 8.0. Data are expressed as mean ± standard error (SE). Statistical evaluation was performed by utilizing one-way analysis of variance (ANOVA), followed by Tukey’s honestly significant difference (HSD) test (significance level: $p < 0.05$).

3. Results

3.1. Gene Cloning and Sequence Analysis of ScinGOBP2

The nucleotide sequence of ScinGOBP2 was confirmed via molecular cloning and sequencing. The ORF of ScinGOBP2 spans 519 nucleotides, encoding a polypeptide of 172 amino acid residues, consistent with earlier reports. The N-terminus of ScinGOBP2 is anticipated to harbor a signal peptide composed of 31 amino acid residues. The mature ScinGOBP2 protein is predicted to have molecular weight of 16.00 kDa and an isoelectric point of 5.16. ScinGOBP2 has a typical six-cysteine signature and exhibits the motif pattern C₁-X₁₅₋₃₉-C₂-X₃-C₃-X₂₁₋₄₄-C₄-X₇₋₁₂-C₅-X₈-C₆ of typical insect OBPs. Multiple sequence alignment illustrated that the ScinGOBP2 protein presented high homology across several lepidopterans, with the highest similarity to *Cydia pomonella* GOBP2 (CpomGOBP2, 84.40%) (Figure 1).

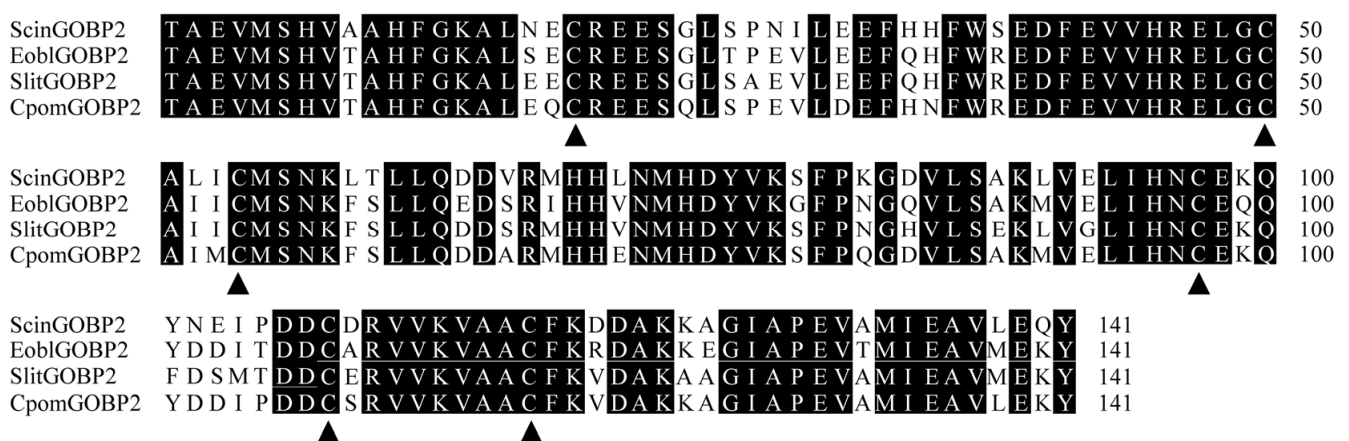


Figure 1. Alignment of amino acid sequences of ScinGOBP2. Only the mature proteins were aligned. The black triangles show the six highly conserved cysteine residues. EoblGOBP2 (*Ectropis obliqua*, ACN29681.1); SlitGOBP2 (*S. litura*, XP_022817877.1); CpomGOBP2 (*C. pomonella*, AFP66958.1).

3.2. Tissue Expression Patterns of *ScinGOBP2*

RT-PCR was utilized to assess the tissue-specific expression patterns of *ScinGOBP2* transcripts across various adult tissues. The presence of β -actin in all tissues served as confirmation the quality of the cDNA templates in each sample. *ScinGOBP2* expression was predominantly observed in the antennae of both sexes, with a reduced intensity of PCR bands observed in male antennae compared to female antennae (Figure 2). The expression level of the *ScinGOBP2* transcript was significantly higher in the antennae compared to other tissues. Specifically, the *ScinGOBP2* transcript was expressed at approximately 18,545 and 8263 times higher in the female and male antennae, respectively, than in each of other body parts. Furthermore, the expression levels in female antennae were approximately 2.2-fold higher than in male antennae (Figure 2).

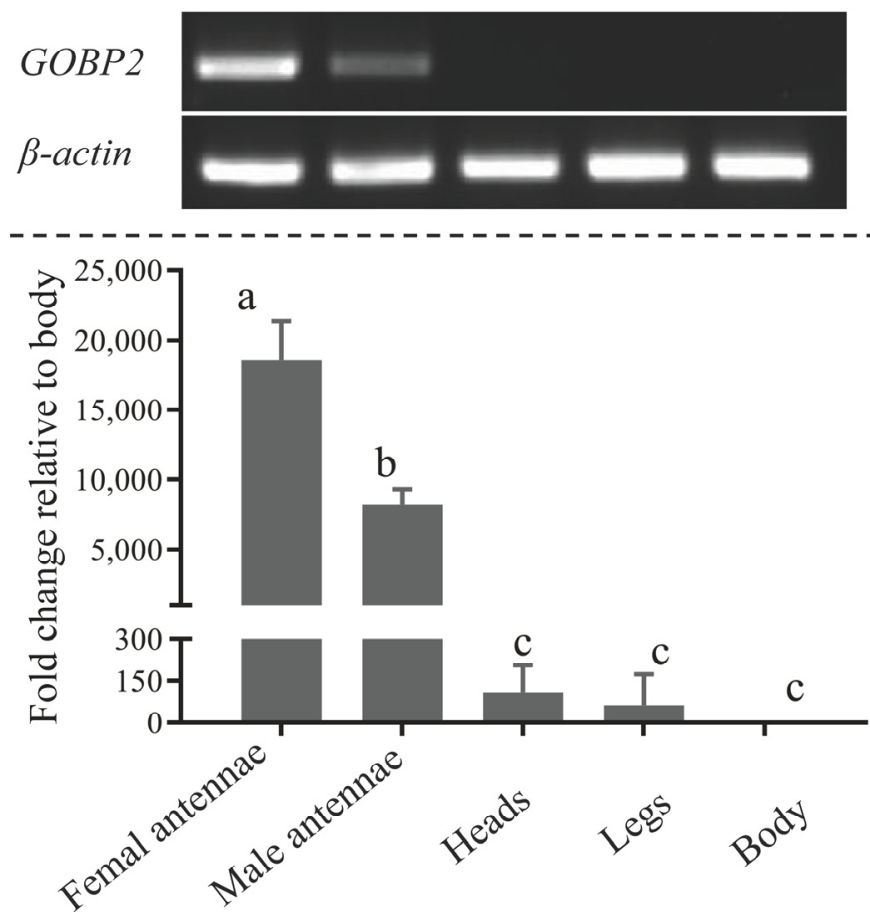


Figure 2. *ScinGOBP2* transcript levels in different tissues were assessed via RT-PCR and qRT-PCR. The error bars represent the standard error, and the different letters indicate significant differences ($p < 0.05$).

3.3. Binding Characteristics of Recombinant *ScinGOBP2*

To identify potential ligands for *ScinGOBP2*, we initially expressed and purified mature *ScinGOBP2* without any modifications. The size and purity of the resultant recombinant protein were verified through SDS-PAGE (Figure S1). Competitive binding assays were performed to investigate its affinity for 27 volatile compounds, using 1-NPN as a fluorescent probe. *ScinGOBP2* binds 1-NPN with good affinity (Figure 3A,B), and the dissociation constant (K_D) for the *ScinGOBP2*/1-NPN complexes was determined to be 2.27 μ M. *ScinGOBP2* exhibited strong binding to geranyl acetone, decanal, *cis*-3-hexenyl *n*-valerate, *cis*-3-hexenyl butyrate, 1-nonene, dipentene, α -pinene, and β -pinene, with K_D values ranging between 2.21 μ M and 14.94 μ M (Figure 3C, Table 1).

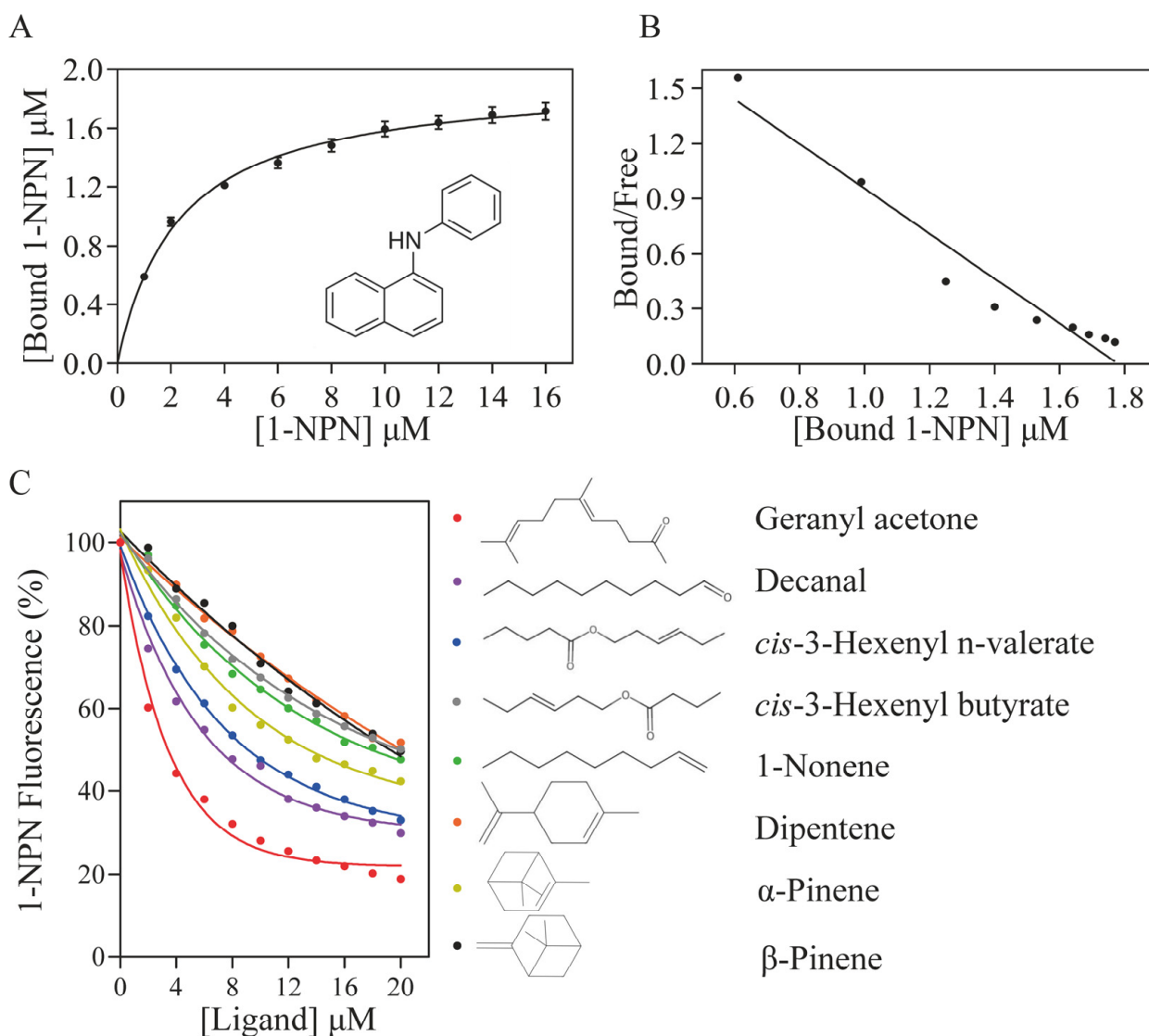


Figure 3. Characteristics of binding interaction exhibited by ScinGOBP2. The affinity of ScinGOBP2 to the fluorescent probe 1-NPN is illustrated through a binding curve (A) and Scatchard plot (B). (C) depicts competitive binding curves that demonstrate the binding of ScinGOBP2 to the selected ligands.

Table 1. Binding affinities of all the tested ligands for ScinGOBP2.

Ligand	Source	CAS Number	Purity (%)	K_D (μM) *
Geranyl acetone	Macklin	3796-70-1	$\geq 98\%$	2.21 ± 0.17
Acetophenone	Macklin	98-86-2	$\geq 99.5\%$	–
<i>cis</i> -3-Hexen-1-ol	Macklin	928-96-1	98%	–
<i>cis</i> -2-Nonen-1-ol	TCI	41453-56-9	$>95.0\%$	–
2-Ethylhexan-1-ol	TCI	104-76-7	$>99.5\%$	–
1-Octanol	TCI	111-87-5	$>99\%$	–
Hexanal	TCI	66-25-1	$>98\%$	–
Nonanal	TCI	124-19-6	$>95\%$	–
Decanal	TCI	112-31-2	$>97\%$	5.07 ± 0.27
3-Methyl-2-butenal	Macklin	107-86-8	98%	–
2-Hexenal	Macklin	6728-26-3	98%	–
Octane	Macklin	111-65-9	$>99\%$	–
<i>cis</i> -3-Hexenyl acetate	Macklin	3681-71-8	98%	–

Table 1. Cont.

Ligand	Source	CAS Number	Purity (%)	K_D (μM) *
<i>cis</i> -3-Hexenyl n-valerate	Macklin	35852-46-1	98%	6.55 \pm 0.18
Ethyl acetate	Macklin	141-78-6	$\geq 99.7\%$	–
Butyl acetate	Macklin	123-86-4	$\geq 99.7\%$	–
Hexyl acetate	TCI	142-92-7	$>99\%$	–
<i>cis</i> -3-Hexenyl butyrate	Macklin	16491-36-4	$\geq 98\%$	14.17 \pm 0.04
Nonanoic acid	Macklin	112-05-0	$>99\%$	–
Capric Acid	Macklin	334-48-5	$>99\%$	–
2-octeno	TCI	111-67-1	$>95\%$	–
1-Nonene	Macklin	124-11-8	95%	12.20 \pm 0.44
Dipentene	Macklin	7705-14-8	95%	14.94 \pm 0.77
Ocimene	Macklin	13877-91-3	$\geq 90\%$	–
α -Pinene	Macklin	80-56-8	98%	9.41 \pm 0.28
β -Pinene	Macklin	127-91-3	$\geq 95\%$	13.19 \pm 0.19
Isoprene	Macklin	78-79-5	$>99\%$	–

* Dissociation constant (K_D) values are reported only where IC_{50} values could be measured. “–” indicates that data are not available.

3.4. Protein Structure Prediction and Molecular Docking

The 3D structure of ScinGOBP2 (Figure S2) was generated using Alphafold2. The protein model underwent a 20 ns MD simulation for energy minimization and protein stabilization. The structural stability of the protein was assessed by calculating the root mean square deviation (RMSD) and root mean square fluctuation (RMSF) (Figure S3). ERRAT and PROCHECK were used to evaluate the qualities of the protein model. The ERRAT results revealed an overall quality factor of 97.85 (Figure S4). Moreover, the Ramachandran plot indicated that 89.2% of the residues were in the most favored region (Figure S5). All the parameters indicated that the 3D modeling of ScinGOBP2 was reasonable and reliable.

The docking analysis revealed that the ligands demonstrated significant binding affinity for ScinGOBP2, with binding energy values ranging from -5.3 to -7.3 kcal/mol (Table 2). Geranyl acetone had the highest interaction energy, marked by a binding energy of -7.3 kcal/mol (Table 2). Following this, dipentene showed notable interaction, with a binding energy of -6.8 kcal/mol, involving π -sigma interactions with the Phe31 residue (Figure 4, Table 2). The Ser75 amino acid residue in ScinGOBP2 was involved in forming hydrogen bonds with decanal, *cis*-3-hexenyl n-valerate, and *cis*-3-hexenyl butyrate (Figure 4). Hydrophobic interactions were observed between all compounds and ScinGOBP2 (Figure 4, Table 2).

Table 2. Docking results for ScinGOBP2 with different ligands.

Ligand	Binding Energy (kcal/mol)	Hydrophobic Interactions
Geranyl acetone	-7.3	Phe52, Phe55, Trp56, Leu71, Ile113, Val130, Val133, Ala134, Phe137
Decanal	-5.7	Trp56, Met24, Val27, Ala28
<i>cis</i> -3-Hexenyl n-valerate	-6.2	Phe31, Phe52, Trp56, Ile113, Val133, Ala134, Phe137
<i>cis</i> -3-Hexenyl butyrate	-5.9	Phe31, Phe52, Trp56, Ile113, Val133, Ala134, Phe137
1-Nonene	-5.3	Val27, Phe52, Val133, Phe137, Ala28, Ile113, Phe31, Ala134
Dipentene	-6.8	Phe52, Trp56, Leu71, Phe137, Ala134, Tyr95, Val27, Ala28
α -Pinene	-6.2	Phe31, Leu71, Ile113, Val130, Val133, Ala134, Phe137
β -Pinene	-6.3	Phe31, Leu71, Ile113, Val130, Val133, Ala134, Phe137

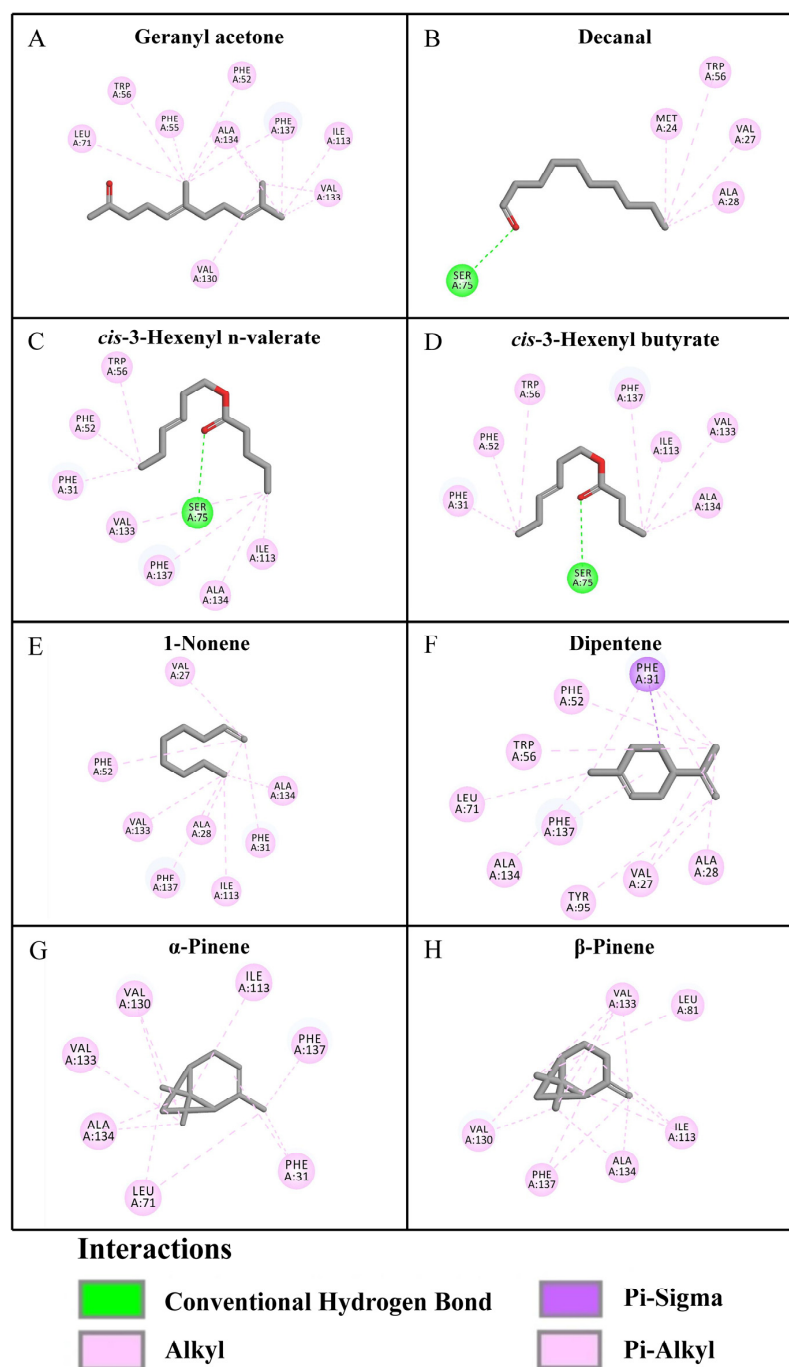


Figure 4. Molecular docking of ScinGOBP2 with (A) geranyl acetone, (B) decanal, (C) *cis*-3-hexenyl n-valerate, (D) *cis*-3-hexenyl butyrate, (E) 1-nonene, (F) dipentene, (G) α -pinene, and (H) β -pinene.

3.5. EAG Recordings

To assess the biological activity of ScinGOBP2 ligands, electrophysiological responses of both female and male *S. cinerearia* to the ScinGOBP2 ligands were evaluated using EAG recordings. All eight volatile compounds elicited EAG responses in the antennae of both sexes of *S. cinerearia* (Figure 5). Females exhibited the most robust EAG response to dipentene, whereas males showed the strongest EAG response to decanal, with mean response values of 0.086 and 0.063 mV, respectively. The EAG responses to all the volatiles, except for dipentene, did not show significant differences between adult males and females.

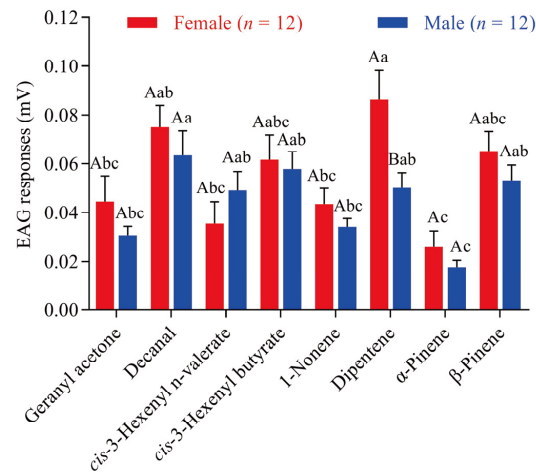


Figure 5. EAG responses of female and male *S. cinerearia* antennae in response to various ligands of ScinGOBP2. Distinct uppercase letters denote significant differences between females and males, while distinct lowercase letters signify significant differences among different chemicals ($p < 0.05$).

3.6. Two-Choice Oviposition Assays

To study the influence of ScinGOBP2 ligands on *S. cinerearia* oviposition, two-choice oviposition assays were conducted in a screened cage (Figure 6A). Females demonstrated a significant preference for laying eggs on gauze areas exposed to decanal, *cis*-3-hexenyl n-valerate, *cis*-3-hexenyl butyrate, and α -pinene compared to other odors (Figure 6B). On the other hand, geranyl acetone, 1-nonene, dipentene, and β -pinene were found to deter *S. cinerearia* from ovipositing (Figure 6B).

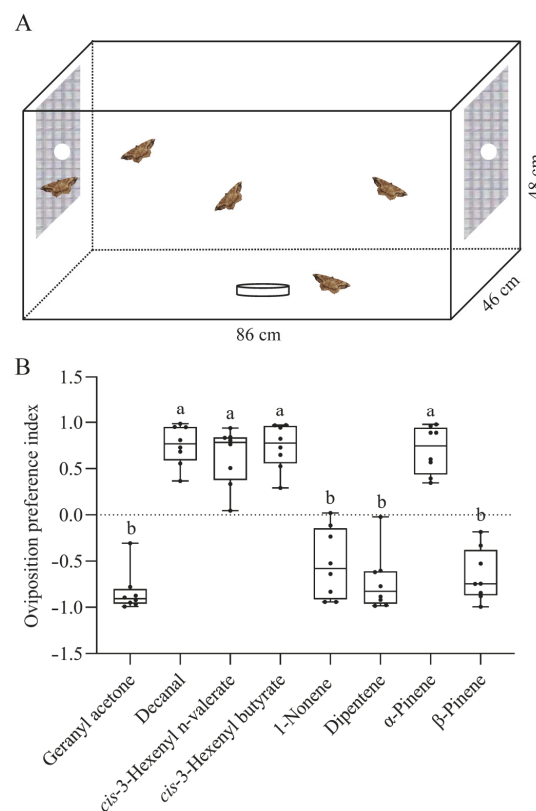


Figure 6. Oviposition preference of female *S. cinerearia* adults for ScinGOBP2 ligands. (A) Schematic diagram of the two-choice oviposition assay. (B) Oviposition preference index of females towards eight compounds. Different letters represent significant differences ($p < 0.05$).

4. Discussion

Moths have a well-developed olfactory system that enables them to utilize different chemical cues for mating and locating a host. Moth PBP/GOBP were the first OBPs studied and have widely documented associations with female sex pheromones and host plant volatile detection. They form a Lepidoptera-specific subfamily within insect OBP gene family, although some non-Lepidoptera OBPs are functionally similar to GOBP/PBP and named PBP or GOBP [13,28]. In this study, the *ScinGOBP2* gene was isolated from *S. cinerearia*. *ScinGOBP2* exhibits six conserved cysteines characteristics of the OBP family and shares a high sequence identity with GOBP2s from other insect species [8,11]. The expression patterns of moth GOBPs, showing sexual dimorphism, vary among different species. For *S. cinerearia*, *ScinGOBP2* was predominantly expressed in the antennae, with significant higher expression levels in females compared to males. This suggests that *ScinGOBP2* might be involved in female-specific behaviors. Female-biased expression has also been observed in several other moth species, such as *Lobesia botrana* [29], *Conogethes pinicolalis* [30], and *Histia rhodope* [31].

The results from the fluorescent binding assays showed that *ScinGOBP2* specifically bound to the tested host plant volatiles, with a high binding affinity (K_D below 15 μ M) for geranyl acetone, decanal, *cis*-3-hexenyl n-valerate, *cis*-3-hexenyl butyrate, 1-nonene, dipentene, α -pinene, and β -pinene. Similar results for GOBP2 binding were found in other moths. *AipsGOBP2* exhibited a high binding affinity for the plant volatiles *cis*-3-hexen-1-ol, oleic acid, dibutyl phthalate, and β -caryophyllene [15], and *OachGOBP2* had a high binding affinity for the host plant volatiles farnesol and α -phellandrene [17]. Prior research has indicated that certain specific amino acids situated within hydrophobic cavities may play a role in the ligand-binding processes of insect OBPs. For example, in *BminOBP3*, V120 is involved in undecanol binding [32], while in *LstiGOBP1*, Thr15 and Trp43 are involved in binding plant volatiles [33]. Molecular docking studies have shown that *ScinGOBP2* strongly interacts with its ligands. Ser75 forms hydrogen bonds with decanal, *cis*-3-hexenyl n-valerate, and *cis*-3-hexenyl butyrate, indicating that it can actively participate in binding in *ScinGOBP2*. However, additional research is required to pinpoint the precise binding sites that mediate the interactions between *ScinGOBP2* and its ligands. Therefore, future experiments involving site-directed mutagenesis will be crucial for addressing this question.

The *ScinGOBP2* ligands can elicit antennal responses in both male and female individuals, indicating that these volatile compounds released by plants might serve as potential semiochemicals for *S. cinerearia*. Plant volatiles such as dipentene, decanal, *cis*-3-hexenyl n-valerate, and geranyl acetone have been shown to act as repellents and/or attractants for some insects [34–38]. In the present study, different *ScinGOBP2* ligands at the same concentrations elicited different behaviors in *S. cinerearia*. Among these volatiles, four (decanal, *cis*-3-hexenyl n-valerate, *cis*-3-hexenyl butyrate, and α -pinene) elicited significant attractant behavioral responses, and four (geranyl acetone, 1-nonene, β -pinene, and dipentene) elicited marked repellent behavioral responses, suggesting that these plant volatiles are vital semiochemicals in communication between female *S. cinerearia* individuals and their host plants in natural habitats. In nature, some male moths may also use plant volatiles to find mates [39–41]. Although *ScinGOBP2* ligands can evoke EAG responses in the antennae of male *S. cinerearia*, there was no apparent correlation between the antennal response to compounds in the EAG analysis and the compounds' behavioral effects [42–44]. Therefore, further studies are needed to determine whether *ScinGOBP2* ligands have behavioral effects on male *S. cinerearia*.

5. Conclusions

We document the female-biased expression and ligand-binding ability of *ScinGOBP2* from *S. cinerearia*, offering insights into the potential olfactory function of GOBP2 in the host-seeking behavior of *S. cinerearia*. Our behavioral trials showed that decanal, *cis*-3-hexenyl n-valerate, *cis*-3-hexenyl butyrate, and α -pinene may represent novel attractants for *S. cinerearia*. Further research is needed to validate the behavioral effects of these

attractants in the field and explore their potential applicability in monitoring and managing *S. cinerearia* populations.

Supplementary Materials: The following supporting information can be downloaded via this link <https://www.mdpi.com/article/10.3390/biology13040274/s1>. Figure S1: SDS–PAGE analysis of recombinant ScinGOBP2. M: molecular weight markers; 1: cell pellet before induction with IPTG; 2: cell pellet after induction; 3: pellet after sonication; 4: supernatant after sonication; 5: protein purified via affinity chromatography, and 6: purified protein after digestion with enterokinase. Figure S2: Three-dimensional (3D) structure of ScinGOBP2. Figure S3: MD simulation results of ScinGOBP2. (A) RMSD plot showing the conformational changes in the protein in 20,000 ps. (B) RMSF plot showing residue fluctuations for 20,000 ps. Figure S4: ERRAT results from the predicted 3D model of ScinGOBP2. Figure S5: PROCHECK results from the predicted 3D model of ScinGOBP2. Table S1: Primers used in this study.

Author Contributions: Conceptualization, J.T. and S.W.; methodology, J.T.; software, Z.W.; validation, S.W., F.Y. and Z.W.; formal analysis, G.Q.; investigation, J.T. and H.L.; resources, S.W.; data curation, J.T.; writing—original draft preparation, S.W.; writing—review and editing, S.W. and A.Z.; visualization, J.T.; supervision, Z.W.; project administration, S.W.; funding acquisition, S.W. and Z.W. All authors have read and agreed to the published version of the manuscript.

Funding: This study was funded by the Promotion and Innovation of Beijing Academy of Agriculture and Forestry Sciences, grant number KJCX20210401, KJCX20240403.

Institutional Review Board Statement: Not applicable.

Informed Consent Statement: Not applicable.

Data Availability Statement: The original contributions presented in the study are included in the article and Supplementary Materials; further inquiries can be directed to the corresponding author.

Conflicts of Interest: The authors declare no conflicts of interest.

References

- Bruce, T.J.A.; Wadhams, L.J.; Woodcock, C.M. Insect host location, a volatile situation. *Trends Plant Sci.* **2005**, *10*, 269–274. [[CrossRef](#)] [[PubMed](#)]
- Metcalfe, R.L.; Kogan, M. Plant volatiles as insect attractants. *Crit. Rev. Plant Sci.* **1987**, *5*, 251–301. [[CrossRef](#)]
- Schoonhoven, L.M.; Van Loon, J.J.A.; Dicke, M. *Insect-Plant Biology*, 2nd ed.; Oxford University Press: New York, NY, USA, 2005.
- Zacharuk, R.Y. Ultrastructure and function of insect chemosensilla. *Annu. Rev. Entomol.* **1980**, *25*, 27–47. [[CrossRef](#)]
- Hansson, B.S.; Stensmyr, M.C. Evolution of insect olfaction. *Neuron* **2011**, *72*, 698–711. [[CrossRef](#)]
- Prelic, S.; Pal Mahadevan, V.; Venkateswaran, V.; Lavista-Llanos, S.; Hansson, B.S.; Wicher, D. Functional interaction between *Drosophila* olfactory sensory neurons and their support cells. *Front. Cell. Neurosci.* **2022**, *15*, 789086. [[CrossRef](#)]
- Leal, W.S. Odorant reception in insects, roles of receptors, binding proteins, and degrading enzymes. *Annu. Rev. Entomol.* **2013**, *58*, 373–391. [[CrossRef](#)]
- Rihani, K.; Ferveur, J.F.; Briand, L. The 40-year mystery of insect odorant-binding proteins. *Biomolecules* **2021**, *11*, 509. [[CrossRef](#)] [[PubMed](#)]
- Ha, T.S.; Smith, D.P. Recent insights into insect olfactory receptors and odorant-binding proteins. *Insects* **2022**, *13*, 926. [[CrossRef](#)]
- Pelosi, P.; Iovinella, I.; Zhu, J.; Wang, G.; Dani, F.R. Beyond chemoreception: Diverse tasks of soluble olfactory proteins in insects. *Biol. Rev. Camb. Philos. Soc.* **2018**, *93*, 184–200. [[CrossRef](#)]
- Zhou, J.J. Odorant-binding proteins in insects. *Vitam. Horm.* **2010**, *83*, 241–272.
- Laue, M.; Steinbrecht, R.A.; Ziegelberger, G. Immunocytochemical localization of general odorant-binding protein in olfactory sensilla of the silkworm *Antheraea polyphemus*. *Naturwissenschaften* **1994**, *81*, 178–180. [[CrossRef](#)]
- Vogt, R.G.; Große-Wilde, E.; Zhou, J.J. The Lepidoptera odorant binding protein gene family, gene gain and loss within the GOBP/PBP complex of moths and butterflies. *Insect Biochem. Mol. Biol.* **2015**, *62*, 142–153. [[CrossRef](#)]
- Nardi, J.B.; Miller, L.A.; Walden, K.K.O.; Rovelstad, S.; Wang, L.; Frye, J.C.; Ramsdell, K.; Deem, L.S.; Robertson, H.M. Expression patterns of odorant-binding proteins in antennae of the moth *Manduca sexta*. *Cell Tissue Res.* **2003**, *313*, 321–333. [[CrossRef](#)] [[PubMed](#)]
- Huang, G.Z.; Liu, J.T.; Zhou, J.J.; Wang, Q.; Dong, J.Z.; Zhang, Y.J.; Li, X.C.; Li, J.; Gu, S.H. Expressional and functional comparisons of two general odorant binding proteins in *Agrotis ipsilon*. *Insect Biochem. Mol. Biol.* **2018**, *98*, 34–47. [[CrossRef](#)] [[PubMed](#)]
- Liu, X.L.; Wu, Z.R.; Liao, W.; Zhang, X.Q.; Pei, Y.W.; Lu, M. The binding affinity of two general odorant binding proteins in *Spodoptera frugiperda* to general volatiles and insecticides. *Int. J. Biol. Macromol.* **2023**, *252*, 126338. [[CrossRef](#)] [[PubMed](#)]

17. Ma, Y.; Li, Y.; Wei, Z.-Q.; Hou, J.H.; Si, Y.X.; Zhang, J.; Dong, S.L.; Yan, Q. Identification and functional characterization of general odorant binding proteins in *Orthaga achatina*. *Insects* **2023**, *14*, 216. [[CrossRef](#)] [[PubMed](#)]
18. Han, W.K.; Wei, Z.Q.; Yang, Y.L.; Liu, X.L.; Yan, Q.; Zhang, J.; Dong, S.L. Roles of GOBP1 in perception of host plant volatiles revealed by CRISPR/Cas9-mediated mutagenesis in *Spodoptera litura*. *J. Appl. Entomol.* **2023**, *147*, 602–610. [[CrossRef](#)]
19. Jing, D.; Prabu, S.; Zhang, T.; Bai, S.; He, K.; Wang, Z. Genetic knockout and general odorant-binding/chemosensory protein interactions, Revealing the function and importance of GOBP2 in the yellow peach moth's olfactory system. *Int. J. Biol. Macromol.* **2021**, *193*, 1659–1668. [[CrossRef](#)]
20. Liu, Z.; Vidal, D.M.; Syed, Z.; Ishida, Y.; Leal, W.S. Pheromone binding to general odorant-binding proteins from the navel orange worm. *J. Chem. Ecol.* **2010**, *36*, 787–794. [[CrossRef](#)]
21. Han, W.K.; Yang, Y.L.; Si, Y.X.; Wei, Z.Q.; Liu, S.R.; Liu, X.L.; Yan, Q.; Dong, S.L. Involvement of GOBP2 in the perception of a sex pheromone component in both larval and adult *Spodoptera litura* revealed using CRISPR/Cas9 mutagenesis. *Insect Biochem. Mol. Biol.* **2022**, *141*, 103719. [[CrossRef](#)]
22. Guo, H.; Guo, P.P.; Sun, Y.L.; Huang, L.Q.; Wang, C.Z. Contribution of odorant binding proteins to olfactory detection of (Z)-11-hexadecenal in *Helicoverpa armigera*. *Insect Biochem. Mol. Biol.* **2021**, *131*, 103554. [[CrossRef](#)] [[PubMed](#)]
23. Shu, W.J.; Tang, J.M.; Chen, Z.Y.; Jiang, Y.S.; Wang, Z.F.; Wei, X. Analysis of genetic diversity and population structure in *Sophora japonica* Linn. in China with newly developed SSR markers. *Plant Mol. Biol. Rep.* **2019**, *37*, 87–97. [[CrossRef](#)]
24. Yu, S.U.N.; Zuo-deng, P.E.N.G. Insights into history culture and value of *Sophora japonica*. *J. Beijing For. Univ. Soc. Sci.* **2018**, *17*, 23–31.
25. Liu, P.; Zhang, X.; Meng, R.; Liu, C.; Li, M.; Zhang, T. Identification of chemosensory genes from the antennal transcriptome of *Semiothisa cinerearia*. *PLoS ONE* **2020**, *15*, e0237134. [[CrossRef](#)] [[PubMed](#)]
26. Zhu, X.Y.; Xu, J.W.; Li, L.L.; Wang, D.Y.; Zhang, M.L.; Yu, N.N.; Purba, E.R.; Zhang, F.; Li, X.M.; Zhang, Y.N.; et al. Analysis of chemosensory genes in *Semiothisa cinerearia* reveals sex-specific contributions for type-II sex pheromone chemosensation. *Genomics* **2020**, *112*, 3846–3855. [[CrossRef](#)] [[PubMed](#)]
27. Yan, G. Releasing Variation and Effects on Human Health of Volatile Organic Compounds from Landscape Trees in Beijing. Ph.D. Thesis, Beijing Forestry University, Beijing, China, 2005.
28. Lescop, E.; Briand, L.; Pernollet, J.C.; Guittet, E. Structural basis of the broad specificity of a general odorant-binding protein from honeybee. *Biochemistry* **2009**, *48*, 2431–2441. [[CrossRef](#)] [[PubMed](#)]
29. Rojas, V.; Jiménez, H.; Palma-Millanao, R.; González-González, A.; Machuca, J.; Godoy, R.; Ceballos, R.; Mutis, A.; Venthur, H. Analysis of the grapevine moth *Lobesia botrana* antennal transcriptome and expression of odorant-binding and chemosensory proteins. *Comp. Biochem. Phys. D Genom. Proteom.* **2018**, *27*, 244. [[CrossRef](#)] [[PubMed](#)]
30. Jing, D.; Zhang, T.; Bai, S.; He, K.; Prabu, S.; Luan, J.; Wang, Z. Sexual-biased gene expression of olfactory-related genes in the antennae of *Conogethes pinicolalis* (Lepidoptera, Crambidae). *BMC Genom.* **2020**, *21*, 244. [[CrossRef](#)] [[PubMed](#)]
31. Yang, H.; Dong, J.; Sun, Y.; Hu, Z.; Lv, Q.; Li, D. Antennal transcriptome analysis and expression profiles of putative chemosensory soluble proteins in *Histia rhodope Cramer* (Lepidoptera, Zygaenidae). *Comp. Biochem. Phys. D Genom. Proteom.* **2020**, *33*, 100654. [[CrossRef](#)]
32. Yang, L.; Tian, X.; Gui, L.; Wang, F.; Zhang, G. Key amino acid residues involved in binding interactions between *Bactrocera minax* odorant-binding protein 3 (BminOBP3) and undecanol. *Insects* **2023**, *14*, 745. [[CrossRef](#)]
33. Yin, J.; Zhuang, X.; Wang, Q.; Cao, Y.; Zhang, S.; Xiao, C.; Li, K. Three amino acid residues of an odorant-binding protein are involved in binding odours in *Loxostege sticticalis* L. *Insect Mol. Biol.* **2015**, *24*, 528–538. [[CrossRef](#)] [[PubMed](#)]
34. Conboy, N.J.A.; Mcdaniel, T.; George, D.; Ormerod, A.; Tosh, C.R. Volatile organic compounds as insect repellents and plant elicitors, An integrated pest management (IPM) strategy for glasshouse whitefly (*Trialetrodes vaporariorum*). *J. Chem. Ecol.* **2020**, *46*, 1090–1104. [[CrossRef](#)]
35. Fan, J.; Zheng, K.; Xie, P.; Dong, Y.; Gu, Y.; Wickham, J.D. Electrophysiological and behavioral responses of *Batocera horsfieldi* Hope to volatiles from *Pistacia chinensis* Bunge. *Insects* **2023**, *14*, 911. [[CrossRef](#)] [[PubMed](#)]
36. Prokopy, R.J.; Phelan, P.L.; Wright, S.E.; Minalga, A.J.; Barger, R.; Leskey, T.C. Compounds from host fruit odor attractive to adult plum curculios (Coleoptera, Curculionidae). *J. Entomol. Sci.* **2001**, *36*, 122–134. [[CrossRef](#)]
37. Zhang, L.; Zhao, M.; Aikeremu, F.; Huang, H.; You, M.; Zhao, Q. Involvement of three chemosensory proteins in perception of host plant volatiles in the tea green leafhopper, *Empoasca onukii*. *Front. Physiol.* **2023**, *13*, 2687. [[CrossRef](#)]
38. Lindmark, M.; Ganji, S.; Wallin, E.A.; Schlyter, F.; Unelius, C.R. Semiochemicals produced by fungal bark beetle symbiont *Endoconidiophora rufipennis* and the discovery of an anti-attractant for *Ips typographus*. *PLoS ONE* **2023**, *18*, e0283906. [[CrossRef](#)]
39. Borrero-Echeverry, F.; Bengtsson, M.; Nakamura, K.; Witzgall, P. Plant odor and sex pheromone are integral elements of specific mate recognition in an insect herbivore. *Evolution* **2018**, *72*, 2225–2233. [[CrossRef](#)]
40. Jarrett, B.J.M.; Miller, C.W. Host plant effects on sexual selection dynamics in phytophagous insects. *Annu. Rev. Entomol.* **2023**, *69*, 41–57. [[CrossRef](#)]
41. Deng, J.Y.; Wei, H.Y.; Huang, Y.P.; Du, J.W. Enhancement of attraction to sex pheromones of *Spodoptera exigua* by volatile compounds produced by host plants. *J. Chem. Ecol.* **2004**, *30*, 2037–2045. [[CrossRef](#)]
42. Gemeno, C.; Leal, W.S.; Mori, K.; Schal, C. Behavioral and electrophysiological responses of the brownbanded cockroach, *Supella longipalpa*, to stereoisomers of its sex pheromone, supellapyrone. *J. Chem. Ecol.* **2003**, *29*, 1797–1811. [[CrossRef](#)]

43. Deletre, E.; Chandre, F.; Williams, L.; Duménil, C.; Menut, C.; Martin, T. Electrophysiological and behavioral characterization of bioactive compounds of the *Thymus vulgaris*, *Cymbopogon winterianus*, *Cuminum cyminum* and *Cinnamomum zeylanicum* essential oils against *Anopheles gambiae* and prospects for their use as bednet treatments. *Parasites Vectors* **2015**, *8*, 316. [[CrossRef](#)] [[PubMed](#)]
44. Robinson, A.; Busula, A.O.; Voets, M.A.; Beshir, K.B.; Caulfield, J.C.; Powers, S.J.; Verhulst, N.O.; Winskill, P.; Muwanguzi, J.; Birkett, M.A.; et al. Plasmodium-associated changes in human odor attract mosquitoes. *Proc. Natl. Acad. Sci. USA* **2018**, *115*, E4209–E4218. [[CrossRef](#)] [[PubMed](#)]

Disclaimer/Publisher’s Note: The statements, opinions and data contained in all publications are solely those of the individual author(s) and contributor(s) and not of MDPI and/or the editor(s). MDPI and/or the editor(s) disclaim responsibility for any injury to people or property resulting from any ideas, methods, instructions or products referred to in the content.